PROBABILISTIC FAULT DISPLACEMENT HAZARD ANALYSIS USING MODEL OF SEISMIC SOURCE CHARACTERISTICS AT THE IKATA SITE BASED ON GUIDELINES FOR SSHAC LEVEL 3

Naoki NISHIZAKA[1], Kozo ONISHI[2], Yoshihiko ISHIKAWA[3],
Masato ONO[4], Jun'ichi MIYAKOSHI[5], Michiharu IKEDA[6],
Takeshi TSUJI[7], Takashi KUMAMOTO[8] and Koji OKUMURA[9]

[1] Member, M. Eng., Shikoku Electric Power Co., Inc. and School of Engineering, University of Tokyo, Kagawa, Japan, nishizaka14981@yonden.co.jp
[2] Member, Dr. Sc., Shikoku Electric Power Co., Inc., Kagawa, Japan, oonishi16286@yonden.co.jp
[3] M. Eng., Shikoku Electric Power Co., Inc., Kagawa, Japan, ishikawa15596@yonden.co.jp
[4] M. Eng., Shikoku Electric Power Co., Inc., Kagawa, Japan, oono16643@yonden.co.jp
[5] Member, Dr. Eng., Ohsaki Research Institute, Inc., Tokyo, Japan, miya@ohsaki.co.jp
[6] Dr. Sc., Shikoku Research Institute, Inc., Kagawa, Japan, m-ikeda@ssken.co.jp
[7] Dr. Sc., Professor, School of Engineering, University of Tokyo, Tokyo, Japan, tsuji@sys.t.u-tokyo.ac.jp
[8] Member, Dr. Sc., Professor, Graduate School of Natural Science and Technology, Okayama University, Okayama, Japan, tkuma@cc.okayama-u.ac.jp
[9] Dr. Sc., Professor Emeritus, Hiroshima University, Hiroshima, Japan, kojiok@hiroshima-u.ac.jp

ABSTRACT: Fault displacement is an important hazard to be considered in the seismic design of structures, along with strong ground motion. In recent years, standards and safety guides for probabilistic fault displacement hazard analysis have been published, and social demand for probabilistic verification of fault displacement underneath critical facilities has increased. However, the practice of this method is very limited worldwide, and there are no reports of its full-scale implementation for a specific structure in Japan. In order to achieve wide application in the future, we should first practice probabilistic fault displacement hazard analysis based on a model with higher accuracy, and then understand the current issues properly. Here, we practice the probabilistic fault displacement hazard analysis using model of seismic source characteristics at the Ikata site based on guidelines for SSHAC Level 3, and report on the specific issues in its application at the practical level, referred to the knowledge obtained from the observation data of the 2016 Kumamoto earthquake.

Keywords: *Probabilistic fault displacement hazard analysis, Median Tectonic Line active fault zone, Distributed fault*

1. INTRODUCTION

As Japan is an earthquake-prone country, the seismic design of structures must consider fault displacement as a hazard together with strong ground motions. At nuclear installations requiring significantly high safety levels, it must be deterministically demonstrated there are no faults that may displace directly underneath critical facilities. However, demonstrating this takes a great deal of time and effort if there are no overlying strata or mineral veins that are suitable for evaluating fault activity. Moreover, when building distributed infrastructure facilities for carbon neutrality, such as pipeline networks for carbon capture and storage or for hydrogen energy use, it may be unrealistic to conduct an exhaustive investigation of underlying faults or avoid active faults, as is done for nuclear facilities.

In 2003, Youngs et al.[1] proposed the probabilistic fault displacement hazard analysis (PFDHA) as a methodology to probabilistically address the issue of fault displacement. The methodology calculates the annual frequency at which the fault displacement on the ground surface exceeds a specified amount at a given site (annual exceedance frequency (AEF)) by using two approaches: the earthquake approach and the displacement approach. The first approach is similar to the probabilistic seismic hazard analysis (PSHA), which models seismic source characteristics such as the magnitude and frequency of occurrence of earthquakes and relates them to the mechanism of earthquake occurrence. On the other hand, the second approach uses the results of direct observation of faults and geological strata of the site under study. Here, the surface ruptures used by the PFDHA can be broadly classified into two types: principal fault, which is closely related to the earthquake source fault, and distributed fault, which appears as secondary or subsidiary fault due to the activities of the principal fault. In this paper, we will carry out an evaluation of distributed fault using the earthquake approach for the Ikata site in the northwestern part of Shikoku in Japan, which was located to avoid areas where fault displacements have been repeatedly observed in new geological strata.

The fault displacement prediction equations shown by Youngs et al.[1] were developed to evaluate seismic damage from normal faults in the United States. In 2011, Petersen et al.[2] and Moss and Ross[3] presented prediction equations for strike-slip and reverse faults, respectively. Additionally, Takao et al. published a series of studies in 2013[4], 2014[5], and 2016[6] that developed prediction equations applying the methodology by Youngs et al.[1] to data on Japan, which has predominantly strike-slip and reverse faults, with the aim of developing PFDHA for use in Japan.

To improve the reliability of fault displacement evaluation in Japan, the Atomic Energy Society of Japan (AESJ) recently published probabilistic risk assessment implementation standards based on PFDHA (hereinafter AESJ Standards)[7]. The Safety Guide for Seismic Hazards by the International Atomic Energy Agency (IAEA)[8], which was revised at about the same time, also recommends PFDHA when there is a possibility that fault displacement may affect the foundation of critical nuclear facilities. Thus, although the tools and standards for implementing PFDHA are available, application has been very limited for nuclear facilities worldwide[9]. To our knowledge, no prior research in Japan has gone beyond studies such as the IAEA benchmark test for the 2016 Kumamoto Earthquake seismic source region (Valentini et al.[10]) and the comparison of hazards at trench excavation sites based on information before and after the earthquake (Inoue et al.[11]) to fully implement PFDHA for specific structures. Hence, to improve the various prediction equations, PFDHA must first be actually applied, even if only on a trial basis[5].

In light of this situation, we believe that PFDHA must first be implemented based on a highly accurate model to be able to assess current issues, with the ultimate goal of widening its range of application in the future. In PFDHA, the earthquake approach uses the same model of seismic source characteristics as PSHA and replaces PSHA's model of ground motion characteristics with a model of fault displacement characteristics. Accordingly, performing PFDHA on a site with highly accurate PSHA models is ideal for our purposes. The first application of the guidelines for Senior Seismic Hazard Analysis Committee (SSHAC) Level 3[12, 13] in Japan was the Ikata SSHAC Project (Kameda et al.[14]), which created a reliable model of seismic source characteristics of the Ikata site (Kumamoto et al.[15]). We therefore believe that applying PFDHA at the site will greatly contribute to development of PFDHA. In this paper, we apply PFDHA to the Ikata site by using the model of seismic source characteristics from the Ikata SSHAC Project and discuss specific issues on its practical use in light of the results as

well as findings from the 2016 Kumamoto Earthquake observation data showing detailed surface rupture distribution over a wide area.

2. SEISMOTECTONICS AROUND THE IKATA SITE AND SEISMIC SOURCES

The Ikata site is located near the Seto Inland Sea (Iyo-nada Sea) in the northwestern part of Shikoku on the continental Eurasian Plate (Amur Plate) and with the oceanic Philippine Sea Plate subducting at the Nankai Trough of the south in the northwest direction (Fig. 1(a)). The Median Tectonic Line (MTL) runs close to the Ikata site and divides the geological structure of southwestern Japan into inner and outer zones. The line starting from western Kii Peninsula to Shikoku is called the Median Tectonic Line active fault zone (MTLAFZ) and corresponds to a right-lateral strike-slip active fault that runs east-northeast and west-southwest (Fig. 1(b)). Aside from the MTLAFZ, the Gotanda, F-21, and other strike-slip active faults running east-northeast to west-southwest are scattered around the Ikata site. The portion of the MTLAFZ called the Iyo-nada Segment[14), 15)] is the active intraplate fault closest to the Ikata site (Fig. 1(b)).
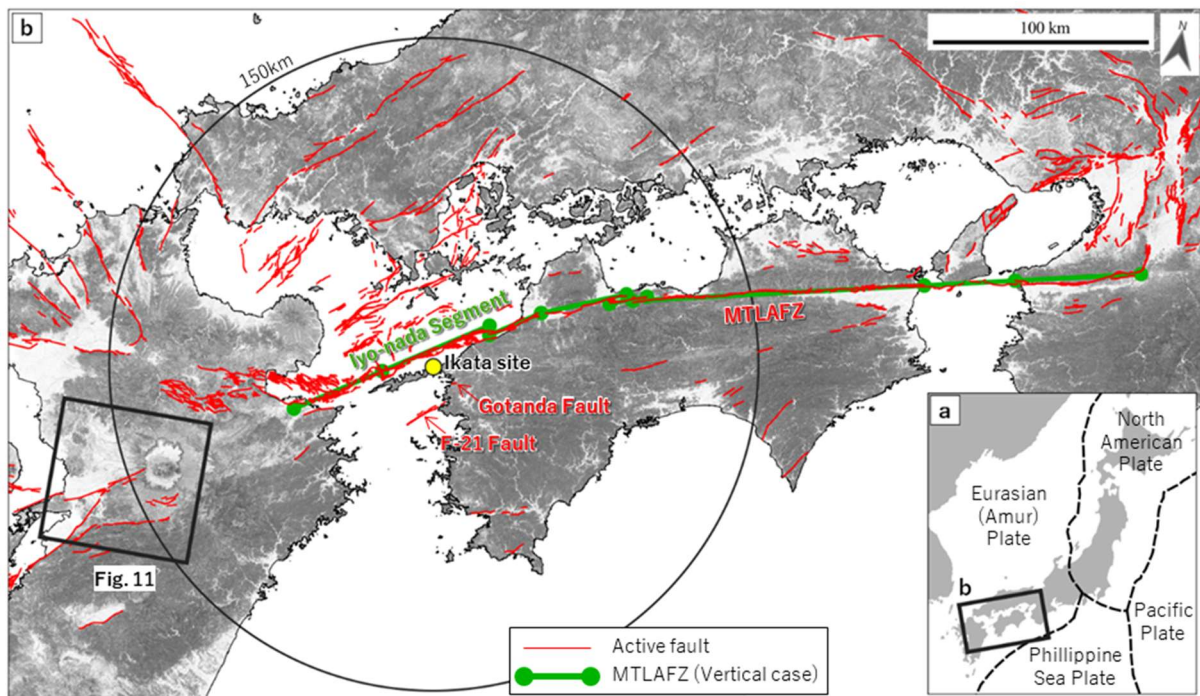

Fig. 1   Distribution of active faults around the Ikata site and segmentation of the MTLAFZ. Active fault distribution and segmentation are based on the Ikata SSHAC Project Final Report[14)].

In the Ikata SSHAC Project, six types of earthquake were used as seismic sources for PSHA, namely (1) MTLAFZ earthquakes, (2) other active intraplate fault earthquakes, (3) the Nankai Trough Megathrust Earthquakes, (4) blind earthquakes in landward plates, (5) blind earthquakes in the Philippine Sea Plate, and (6) earthquakes smaller than the characteristic magnitude of active intraplate faults[15)]. Based on the lessons learned from the 2016 Kumamoto Earthquake foreshock (M_J 6.5 earthquake that struck on April 14, 2016) with a seismic intensity of 7 on the Japanese scale, earthquakes smaller than the characteristic magnitude of active intraplate faults are defined here as the "earthquakes whose activities are difficult to detect from surface evidence" given by the Earthquake Research Committee of the Headquarters for Earthquake Research Promotion (HERP)[16)] plus the earthquakes that are magnitudes smaller than the characteristic magnitude of active intraplate faults that do not leave traces on the surface, in order to eliminate any "gaps" in the earthquake hazard evaluation. Thus,

earthquakes occurring on the Iyo-nada Segment are targeted in view of their effect on PSHA[15].
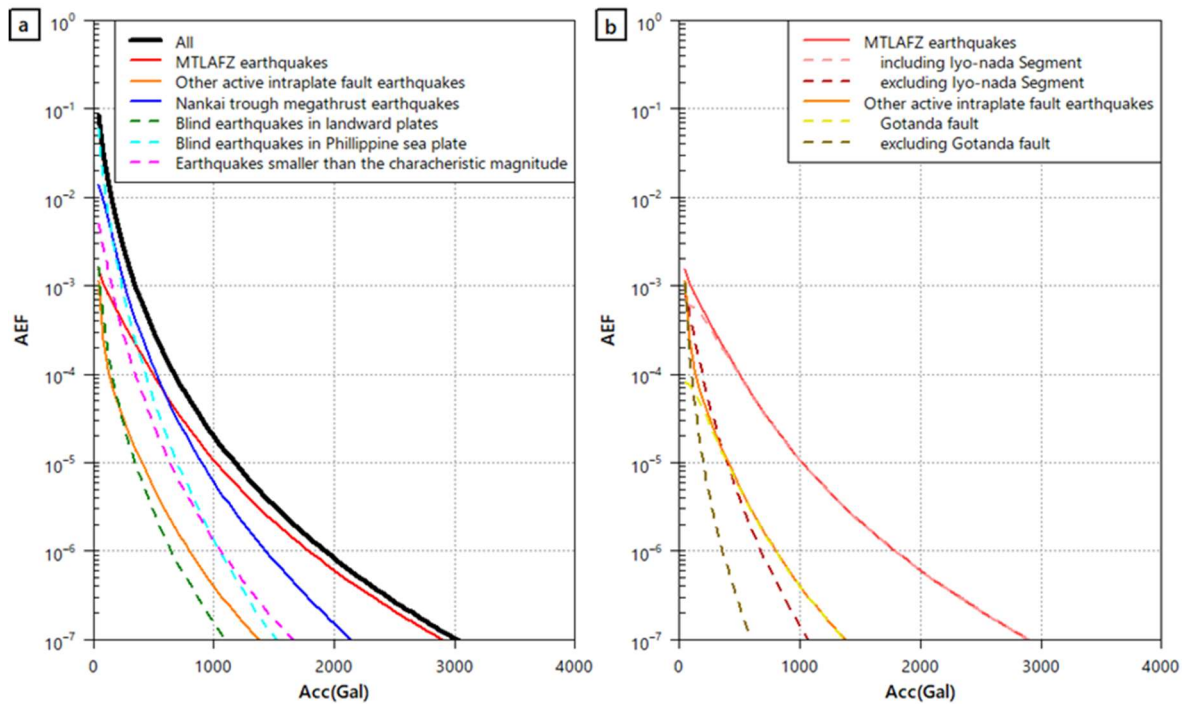

Fig. 2 PSHA results. (a) Seismic hazard curves of each seismic source. (b) Seismic hazard curves of MTLAFZ earthquakes (including and excluding the Iyo-nada Segment) and of other active intraplate fault earthquakes (separated into the Gotanda fault and other than the Gotanda fault). Representative horizontal ground motion results for a period of 0.02 s are shown. Prepared based on the Ikata SSHAC Project Final Report[14] and Fujiwara et al.[18].

According to the AESJ Standards[7], sensitivity analyses that change the values of parameters affecting PSHA are considered useful as a preliminary analysis for PFDHA. Hence, while referring to the seismic sources that significantly affect the PSHA, we also examine seismic sources based on seismotectonics for the PFDHA. Figure 2 shows the weighted mean PSHA results for each seismic source calculated in the Ikata SSHAC Project. Over the range of large acceleration levels with horizontal ground motions exceeding 500 Gal (cm/s^2), MTLAFZ earthquakes have the largest effect (Fig. 2(a)); for MTLAFZ earthquakes, the effect of the Iyo-nada Segment closest to the Ikata site is dominant (Fig. 2(b)). Looking at intraplate crustal seismic sources for use in PFDHA, over the range of low acceleration levels, aside from MTLAFZ earthquakes (characteristic earthquakes), the effect of earthquakes smaller than characteristic magnitude of active intraplate faults occurring at the Iyo-nada Segment can also be observed, while the effect of the remaining seismic sources—blind earthquakes in landward plates and other active intraplate fault earthquakes—were little overall. Blind earthquakes in landward plates are, in the first place, earthquakes occurring in areas where active faults have not been identified beforehand because no traces of fault displacement remain on the surface. Moreover, the Ikata site is on a zone that is subject to efficient strain release by the mature MTLAFZ with low seismic activity[15]; and according to Toda[17], there are few small-scale faults along mature major faults such as the MTLAFZ, so their effect on PFDHA was judged to be negligibly small. For other active intraplate fault earthquakes, the Gotanda fault, which is the second closest to the Ikata site after the MTLAFZ, dominates the PSHA results, although its hazard is notably smaller than the hazard from the Iyo-nada Segment (Fig. 2(b)). The Gotanda fault is a short, isolated, and presumed active fault with a length of about 2 km, for which there is an epistemic uncertainty on whether it is active with 0.5:0.5 weights for active to non-active[15], so its hazard level for PFDHA was judged to be significantly lower compared to the Iyo-nada Segment. Based on these PSHA results and the seismotectonic characteristics, and after eliciting the opinions of

experts in relevant fields, we determined that the AEF of fault displacement at the Ikata site can be represented by the sum of characteristic earthquakes and earthquakes smaller than the characteristic magnitude of active intraplate faults occurring on the Iyo-nada Segment; these seismic sources were used for the PFDHA.

3. ANALYSIS MODELS

The seismic sources for the Ikata site PFDHA are characteristic earthquakes and earthquakes smaller than characteristic magnitude of active intraplate faults occurring on the Iyo-nada Segment. The PFDHA model framework consists of a seismic source characterization model and a fault displacement characterization model. The former follows the Ikata site seismic source characterization model based on guidelines for SSHAC Level 3[14), 15)] without modification, and is equivalent to Expert Utilization Level 3 of the AESJ Standards[7)]. On the other hand, for the latter, given that the model is simple because of the limited number of fault displacement prediction equations currently available, we constructed logic trees and set weights based on the opinions of five experts on active faults, three experts on prediction equations, and three experts involved in developing fault displacement hazard standards. This process is equivalent to Expert Utilization Level 2. The components of the PFDHA model are broadly classified and described below. For details on logic trees and the basis for setting the Ikata site seismic source characterization model based on SSHAC Level 3 guidelines, see Kumamoto et al.[15)] and Ikata SSHAC Project Final Report[14)].

3.1 Seismic source characterization model

3.1.1 Seismic source characterization model for characteristic earthquakes occurring on the Iyo-nada Segment
(1) Modeling the location and geometry as well as magnitude
The logic tree for location and geometry of characteristic earthquakes occurring at the Iyo-nada Segment consists of the planar position, segmentation, depths of the fault plane top and bottom, fault dip angle at deep and shallow sections, and the shortest distance from the principal fault (Fig. 3).
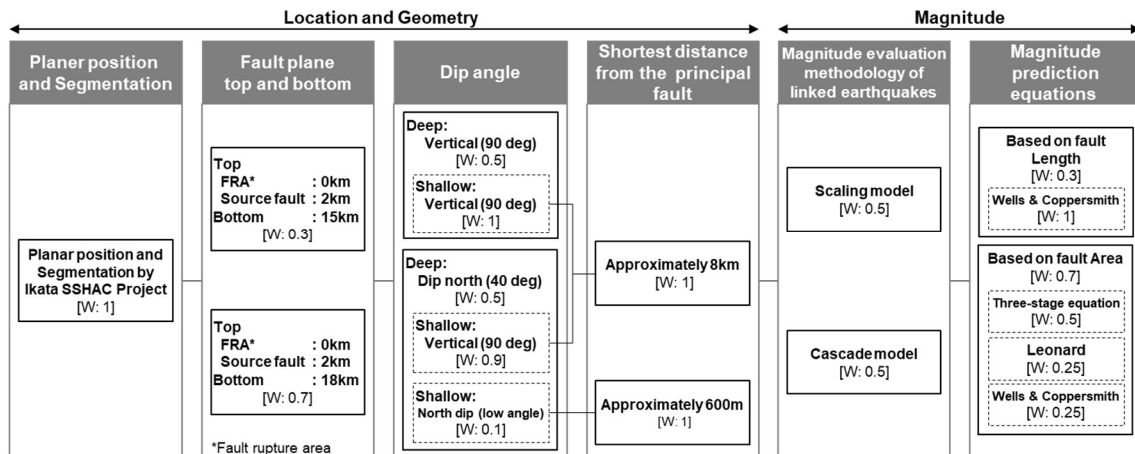

Fig. 3 Logic tree for location and geometry as well as magnitude of characteristic earthquakes occurring on the Iyo-nada Segment. Edited based on the Ikata SSHAC Project Final Report[14)]. W indicates the abbreviation for weight.

Planar position refers to the surface distribution of active faults. At the Iyo-nada Sea offshore of the Ikata site, since the principal fault on the MTLAFZ cuts up through the sediment layer to the seafloor at a high angle (nearly vertical) approximately 8 km offshore, the earthquake source fault has also been set

to run across approximately 8 km offshore (Fig. 4). Active fault groups south of this principal fault (5–8 km offshore of the Ikata site) are considered as distributed fault that appeared as a result of the activity of the principal fault[15]. From 5 km offshore, no active faults have been found in the site vicinity in the southward direction (Fig. 1(b)). The MTLAFZ is a long active fault extending from the Kii Peninsula to Oita and was divided into eight segments, which includes the Iyo-nada Segment (54 km long), based on the concept of earthquake, geometric, and behavioral segments (Japan Society of Civil Engineers[19]). The depth of the top of the fault rupture region used for calculating magnitude is 0 km (ground surface), while the depth of the top of the earthquake source fault that produces short-period strong ground motions is 2 km. The depths of the fault rupture region bottom and earthquake source fault bottom coincide at 15 km and 18 km, with weights of 0.3:0.7. For fault dip angles at sections deeper than 2 km, one branch is vertical (90 deg), which is typical for strike-slip faults, and the other dips north (40 deg), which aligns with the MTL as a geological boundary, with weights set to be equal (0.5:0.5). For fault dip angles at shallow sections shallower than 2 km, the fault dip is basically vertical (90 deg). However, when the deep fault is north-dipping (40 deg), a weight of 0.1 is given to a dip north (low angle) at the shallow section corresponding to a low-angled geological boundary of approximately 15 deg. Although there is no data to support such low-angled geological boundary activity, there are some opinions suggesting its possibility. The branch expresses the range of "center, body and range of technically defensible interpretations" (CBR of TDI), taking into account the fact if the fault strength and friction coefficient are considerably small, the possibility of a low-angle strike-slip cannot be completely ruled out[14]. The shortest distance from the principal fault depends on the fault dip angle setting at the shallow section (Figs. 3 and 4), and is approximately 8 km for the vertical dip (90 deg) and approximately 600 m for the north dip (low angle).
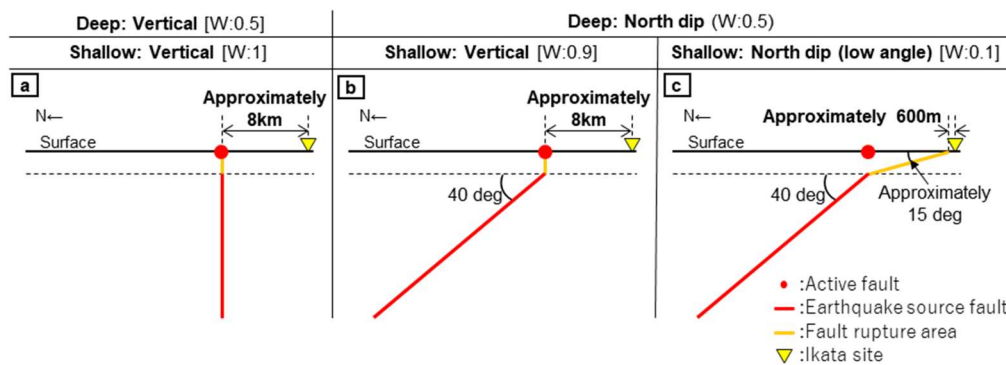

Fig. 4 Schematic diagram of fault dip angles on the Iyo-nada Segment. Edited based on the Ikata SSHAC Project Final Report[14]. W indicates the abbreviation for weight.

The logic tree for the magnitude of characteristic earthquakes occurring at the Iyo-nada Segment consists of the methodology for evaluating the magnitude of linked earthquakes and the earthquake scaling prediction equation (Fig. 3). Since the MTLAFZ is long, when considering characteristic earthquakes occurring at the Iyo-nada Segment, earthquake magnitudes must be calculated for 14 cases, from the case where the Iyo-nada Segment alone ruptures to the case where all eight segments rupture together. For the magnitude evaluation methodology of linked multi-segment earthquakes, one branch is the scaling model, which calculates the seismic moment from the total length or total area of the fault until the applicable limit of the earthquake scaling prediction equation, and the other branch is the cascade model, which calculates the seismic moment from the length or area of each segment regardless of their linkage with weights set to be equal (0.5:0.5). The parameters used to calculate the earthquake scaling prediction equation are fault length and fault area, with weights set at 0.3:0.7. The equation by Wells and Coppersmith[20] was applied with a weight of 1 for the prediction equation calculated using fault length. For the prediction equation calculated using fault area, there are three branches: the three-stage equation that uses Somerville et al.[21], Irikura and Miyake[22], or Murotani et al.[23] depending on the fault area, the equation by Leonard[24], which has been used many times in SSHAC and other projects

worldwide, and the equation by Wells and Coppersmith[20], with weights set at 0.5:0.25:0.25.

(2)   Modeling the probability of occurrence

The logic tree for the probability of occurrence of characteristic earthquakes on the Iyo-nada Segment consists of the methodology for evaluating mean recurrence interval, the time-dependent or time-independent occurrence models (update process (Brownian Passage Time (BPT) distribution) and Poisson process), the latest faulting event, the aperiodicity parameter, the mean slip rate, the displacement per event, and the methodology for evaluating seismic linkage (Fig. 5).
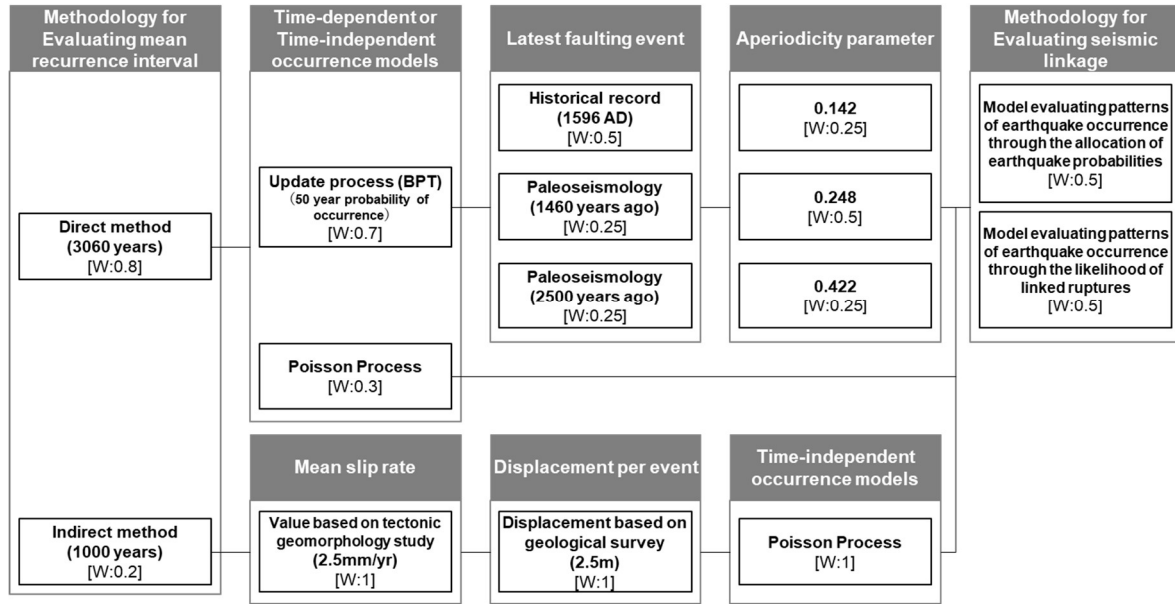
Fig. 5   Logic tree for the probability of occurrence of characteristic earthquakes on the Iyo-nada Segment. Edited based on the Ikata SSHAC Project Final Report[14]. W indicates the abbreviation for weight.

There are two methodologies for evaluating mean recurrence interval: the direct method using 3060 years of historical seismicity obtained from geological surveys, and the indirect method using 1000 years calculated with mean slip rate (2.5 mm/yr) and displacement per event (2.5 m), with weights set at 0.8:0.2. The time-dependent or time-independent occurrence model has two branches. The update process (BPT distribution) can reflect information on the latest faulting event, taken from geological surveys and historical records, in the probability of occurrence, while the Poisson process calculates the probability of occurrence by using only the mean recurrence interval. Their respective weights are 0.7:0.3 when the mean recurrence interval is derived from the direct method, while the weight of the Poisson process is 1 when the mean recurrence interval is derived from the indirect method. For the latest faulting event, there are three branches: 1596 AD when the Keicho-Iyo Earthquake caused a rupture up to the fault at the Iyo-nada Sea, 1460 years ago based on boring surveys of the western edge of the adjacent segment to the east, and 2500 years ago, with weights set at 0.5:0.25:0.25. For aperiodicity parameters, 0.25:0.5:0.25 weights were respectively given to the branches 0.142, 0.248, and 0.422, which were calculated based on the faulting history of the MTLAFZ. Based on the above model, the 50-year probability of occurrence at the Iyo-nada Segment ranges from nearly 0 to a maximum of around 0.05. Additionally, for the methodology to evaluate linkage, one branch is a model evaluating patterns of earthquake occurrence through the allocation of earthquake occurrence probabilities, which is the latest methodology for active intraplate faults given by HERP[25]. The other branch is a new model evaluating patterns of earthquake occurrence through the likelihood of linked ruptures, proposed by Kumamoto et al.[15] with a view of applying it to the MTLAFZ earthquakes based on the Working Group on California Earthquake Probabilities[26], with both models having equal weights (0.5:0.5). Through this model, 63 cases of single/linked rupture patterns are assumed through the combination of 14 different

seismic sources, from the case when the Iyo-nada Segment alone ruptures to the case when all eight segments rupture together.

3.1.2 Seismic source characterization model for earthquakes smaller than characteristic magnitude of active intraplate faults occurring on the Iyo-nada Segment

The logic tree for location and geometry of earthquakes smaller than characteristic magnitude of active intraplate faults occurring at the Iyo-nada Segment consists of the layout of seismic sources and the shortest distance from the principal fault (Fig. 6). For the layout of seismic sources, fault planes corresponding to the magnitude of the earthquake are uniformly distributed within the earthquake source fault plane at the Iyo-nada Segment. Here, earthquakes smaller than characteristic magnitude of active intraplate faults are earthquakes with small displacements that make it difficult to detect traces in trench surveys etc. even if they cause surface ruptures. Focusing on visible displacements, we only considered seismic sources whose fault planes are located at the top of the earthquake source fault and set the shortest distance to the principal fault as the distance from the surface projection of the top of the fault plane.

The logic tree for magnitude and probability of occurrence of earthquakes smaller than characteristic magnitude of active intraplate faults occurring at the Iyo-nada Segment consists of the maximum magnitude, frequency of occurrence Gutenberg–Richter law (G–R law), and time-independent occurrence model. The maximum magnitude Mw is 6.3. Based on the fact that in magnitude-frequency distributions of characteristic earthquakes and all other earthquakes, the maximum magnitude of the latter is generally smaller 1–2 than the former, we have judged and set M as smaller than that of characteristic earthquakes by 1. For the frequency of occurrence (G–R law), the frequency of the maximum magnitude earthquake is the same as the frequency of the characteristic earthquake (for the mean recurrence interval at the Iyo-nada Segment, 3060 years with the direct method, 1000 years with the indirect method). For earthquakes less than the maximum magnitude, the frequency of occurrence is set for each magnitude assumed to follow the G–R law with a b-value of 1. The Poisson process was adopted for the time-independent occurrence model of earthquake occurrence.
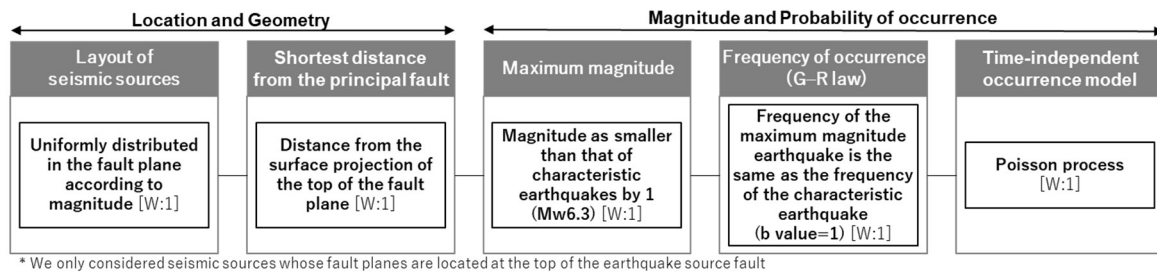

Fig. 6 Logic tree for earthquakes smaller than characteristic magnitude of active intraplate faults occurring at the Iyo-nada Segment. Edited based on the Ikata SSHAC Project Final Report[14]. W indicates the abbreviation for weight.

3.2 Fault displacement characterization model

The logic tree for the fault displacement characterization model of characteristic earthquakes and earthquakes smaller than characteristic magnitude of active intraplate faults occurring on the Iyo-nada Segment consists of the probability of occurrence of the principal fault (P_{1p}), the probability of occurrence of the distributed fault (P_{2d}), and the probability of exceedance of the distributed fault displacement (P_{3d}) (Fig. 7). The probability of occurrence of the principal fault (P_{1p}) and the probability of occurrence of the distributed fault (P_{2d}) are terms related to the earthquake location (shortest distance from the principal fault) in the seismic source characterization model, whereas the probability of exceedance of the distributed fault displacement (P_{3d}) is a parameter related to the magnitude in the seismic source characterization model. Multiplying these parameters by the probability of earthquake

occurrence in the seismic source characterization model provides the AEF of fault displacement at distributed faults (see Appendix 1).

Probability of occurrence of the principal fault (P1p)	Probability of occurrence of the distributed fault (P2d)	Probability of exceedance of the distributed fault displacement (P3d)		
		Distributed fault displacement prediction equation	Relationship between Magnitude and mean Displacement of the principal fault	Variability and Probability distribution of the variation
Characteristic earthquake **Approximately 8km*** **P1p=1 [W:1]** **Approximately 600m*** **P1p= 0.001 [W:1]**	**Approximately 8km or more*** Takao et al. (2014)[5] [W:0.9] Petersen et al.[2] [W:0.1]	Takao et al. (2016)[6] [W:1] Petersen et al.[2] [W:1]	Wells and Coppersmith[20] (All type) Wells and Coppersmith[20] (strike slip)	Wells and Coppersmith[20] (All type) Wells and Coppersmith[20] (strike slip)
Earthquakes smaller than the characteristic magnitude Takao et al. (2013)[4] [W:1]	**Approximately 600m*** Takao et al. (2014)[5] [W:0.5] Petersen et al.[2] [W:0.5]	Takao et al. (2016)[6] [W:1] Petersen et al.[2] [W:1]	Wells and Coppersmith[20] (All type) Wells and Coppersmith[20] (strike slip)	Wells and Coppersmith[20] (All type) Wells and Coppersmith[20] (strike slip)

* Shortest distance from the principal fault

Fig. 7 Logic tree for fault displacement characteristics of earthquakes occurring on the Iyo-nada Segment. W indicates the abbreviation for weight.
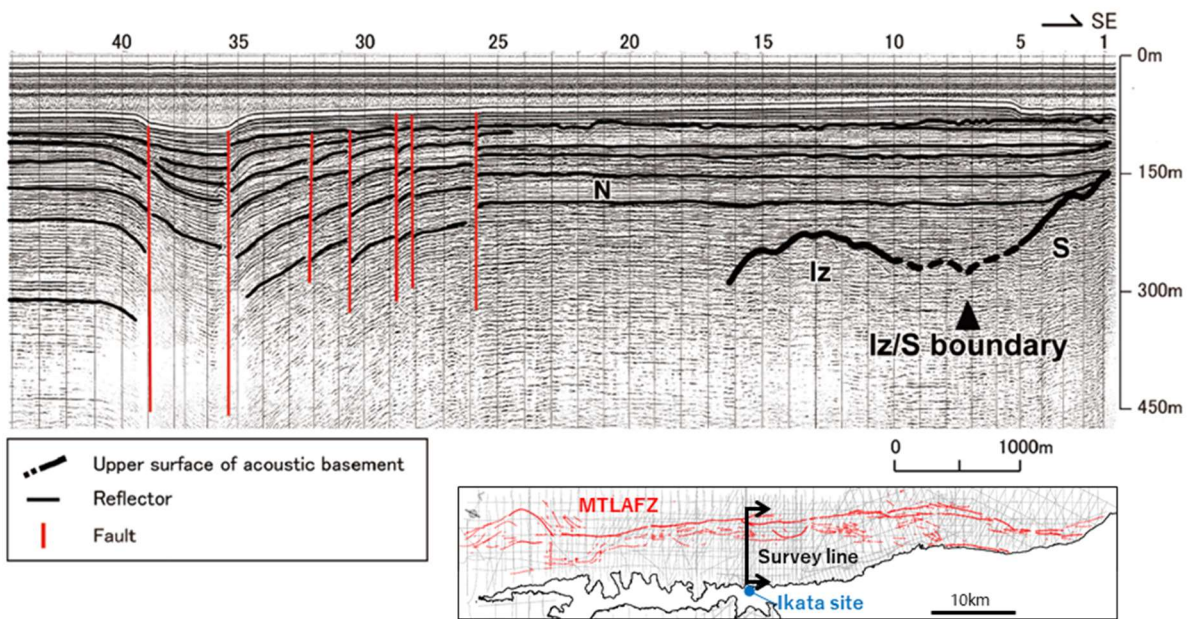

Fig. 8 Interpretation profile of water gun single-channel acoustic exploration record along the coast of the Ikata site, which is taken from Fig. 8(b) of Takahashi et al.[27] with the position of the survey line added. Acoustic exploration record aspect ratio is 1:7 (depth scale is magnified 7 times). The geological boundary (Iz/S) is between the Izumi fault group (Iz) and Sambagawa metamorphic rocks (S). In the northwestern section of the survey line, a high-angled fault group (MTLAFZ) providing clear displacements to the Neogene and Quaternary sediments (N) that reach the seabed has been observed. In contrast, the Neogene and Quaternary sediments covering the geological boundary at the southeastern section of the survey line are almost horizontal.

The probability of occurrence of the principal fault (P_{lp}) is the probability that principal fault displacement ruptures the surface with active fault movement[4]. The MTLAFZ passing through approximately 8 km north of the Ikata site is clearly an active fault that reaches the surface (Fig. 8). The depth of the fault rupture region's top end for the characteristic earthquake is 0 km (ground surface), so there is no need to set other branches[15]. Hence, when the shortest distance from the principal fault is approximately 8 km (that is, the principal fault at the shallow section is vertical) (Figs. 4(a) and 4(b)), the principal fault will always rupture the surface for characteristic earthquakes ($P_{lp} = 1$). On the other hand, when the shortest distance from the principal fault is approximately 600 m, the low-angled northern dip of the geological boundary at the shallow section becomes the principal fault (Fig. 4(c)). Using offshore acoustic exploration records at the shallow geological boundary, Takahashi et al.[27] showed that no activity can be observed after the Quaternary period (Fig. 8). In light of the definition of active faults given in the Active Faults in Japan (revised edition)[28] as faults that have been repeatedly moving in recent geological periods and are presumed to continue to be active in the future, this geological boundary at the shallow section is not an active fault. Even in light of the definition of capable faults that require verification of fault displacement given in the IAEA Safety Guide[8], which states that an assessment of capable faults is appropriate if there is evidence of past activities since the Upper Pleistocene in regions with short earthquake recurrence intervals such as Japan, this shallow geological boundary is not a capable fault. For the case where this shallow geological boundary is the principal fault (the shortest distance from the principal fault is approximately 600 m) (Fig. 4(c)), no activity after the Quaternary period has been observed for the earthquake source fault recurrence intervals from 1000 to 3060 years (Fig. 5). Hence, we set $P_{lp} = 0.001$, assuming that from the engineering perspective the principal fault has not ruptured the ground surface during the past 1000 characteristic earthquakes, and confirmed the effect on fault displacement hazard when $P_{lp} = 0.01$ through sensitivity analysis. For earthquakes smaller than characteristic magnitude of active intraplate faults, we used the prediction equation by Takao et al. (2013)[4], which was developed by a regression analysis of earthquake magnitudes and probability of principal faults in Japan.

The probability of occurrence of the distributed fault (P_{2d}) is the probability that distributed fault displacement appears at a distance from the principal fault when the principal fault ruptures the surface. The prediction equations have been proposed in which the rate of occurrence decreases with greater distance from the principal fault[4]. For equations that can be applied to strike-slip faults, there are the prediction equation by Petersen et al.[2], which is based on earthquake data from strike-slip faults around the world including Japan, the prediction equation by Takao et al. (2013)[4], which is based on earthquake data from strike-slip and reverse faults in Japan, and the prediction equation by Takao et al. (2014)[5], which added model experiments and numerical analyses to the prediction equation by Takao et al. (2013)[4] to improve the reliability of the equation. In this paper, we used the prediction equations by Petersen et al.[2] and Takao et al. (2014)[5]. Here, the proposed equations for calculating the probability of occurrence of the distributed fault (P_{2d}) are dependent on the earthquake magnitude or grid size used during analysis, although the effect of earthquake magnitude is considered smaller than that of grid size[5]. Accordingly, we adopted the equations dependent on grid size and followed the calibration method given by the U.S. Nuclear Regulatory Commission (2012)[29]. After calculating with the prediction equation by Petersen et al.[2] using 200 m x 200 m cell sizes and with the prediction equation by Takao et al. (2014)[5] using 250 m x 250 m, we calibrated with an area ratio equivalent to the value for 160 m x 160 m, which corresponds to the area of critical seismic-resistant facilities at the Ikata site (see Appendix 2 and Fig. A-1(a)). Given that the prediction equation by Petersen et al.[2] is recommended for use only up to 2 km away from the principal fault because of the uncertainty of triggering displacements on other faults, and that the shortest distance to the principal fault at the site is approximately 8 km, the prediction equation by Petersen et al.[2] is basically out of its application range. However, in view of the fact that a prediction equation applicable to strike-slip faults has not been established yet, we decided to treat the variability of the prediction equations as epistemic uncertainty and set both prediction equations as branches, based on the same approach of setting branches for earthquake scaling prediction equations by Kumamoto et al.[15]. For setting weights, Fujiwara et al.[18] considered the uncertainty of the median value by setting the weight of the ground motion prediction equation, which is essentially not applicable to PSHA at the

Ikata site based on guidelines for SSHAC Level 3, to 1/9. Following this approach, we set the weights of prediction equations by Petersen et al.[2] and Takao et al. (2014)[5], to 0.1:0.9. On the other hand, when the shortest distance from the principal fault is approximately 600 m, we set the weights of the prediction equations by Petersen et al.[2] and Takao et al. (2014)[5] to 0.5:0.5. For the approach to setting weights for the case where the shortest distance from the principal fault is 8 km or more for earthquakes smaller than characteristic magnitude of active intraplate faults, the same approach for the case where the shortest distance from the principal fault is approximately 8 km for characteristic earthquakes, was used.

The logic tree for probability of exceedance of the distributed fault displacement (P_{3d}) consists of the distributed fault displacement prediction equation, the relationship between magnitude and mean displacement of the principal fault, and the variability and probability distribution of the variation. The displacement of distributed faults is derived from the prediction equation normalized with respect to the principal fault displacement, using the prediction equation by Petersen et al.[2] as well as the series of studies by Takao et al.[4]–[6] that ends with the revision of the probability density function applying maximum likelihood estimation in Takao et al.[6] (see Appendix 2 and Fig. A-1 (b)). Here, we emphasized consistency with the calculations for the probability of occurrence of the distributed fault (P_{2d}): when the prediction equation by Petersen et al.[2] is used, the prediction equation by Petersen et al.[2] is also used for the distributed fault displacement with a weight of 1, and when the prediction equation by Takao et al. (2014)[5] is used, the prediction equation by Takao et al. (2016)[6] is used with a weight of 1. For the relationship between magnitude and mean displacement of the principal fault, as well as the variability and probability distribution of the variation, we followed the models by Petersen et al.[2] and Takao et al. (2016)[6]: when the prediction equation by Petersen et al.[2] is used for the distributed fault displacement, the relationship for strike-slip faults by Wells and Coppersmith[20] (lognormal distribution with a variance of 0.28) is used, and when the prediction equation by Takao et al. (2016)[6] is used for the distributed fault displacement, the relationship for all fault types by Wells and Coppersmith[20] (lognormal distribution with a variance of 0.36) is used.

4. ANALYSIS RESULTS

4.1 Fault displacement hazard analysis results

Figure 9 shows the results of the PFDHA, which used a combination of a seismic source characterization model and a fault displacement characterization model with different levels of expert utilization. The effects of the latter model must be carefully noted since it has a low level of expert utilization and lower accuracy. When activity of the MTLAFZ (Iyo-nada Segment) is considered, the annual frequency of fault displacements occurring directly below critical seismic-resistant facilities at the Ikata site is about 1×10^{-7} for both mean and median values, with the mean slightly larger than the median. Moreover, for displacements over 0.1 m, the AEF exponentially declines with increasing displacement (Fig. 9(a)). When the results of the mean value are broken down into characteristic earthquakes and earthquakes smaller than characteristic magnitude of active intraplate faults, the hazard curve for characteristic earthquakes is nearly identical to the hazard curve showing the mean for all earthquakes for displacements over 0.01 m (Fig. 9(b)). Hence, for the fault displacement hazard, the effect of characteristic earthquakes dominates, and its hazard curve diverges greatly from the hazard curve of earthquakes smaller than characteristic magnitude of active intraplate faults as the displacement increases (Fig. 9(b)). This tendency persists when the median value is broken down into characteristic earthquakes and earthquakes smaller than characteristic magnitude of active intraplate faults, although their curves are close to each other at 0.01 m (Fig. 9(c)). Looking at the AEF at a displacement of 0.01 m for characteristic earthquakes, the mean of 1.7×10^{-7} (Fig. 9(b)) is larger than the median of 5.6×10^{-8} (Fig. 9(c)), with the graph showing larger mean values in general. This result may be due to the fact that remarkably low-frequency events with large displacements were also included in some branches of characteristic earthquakes.
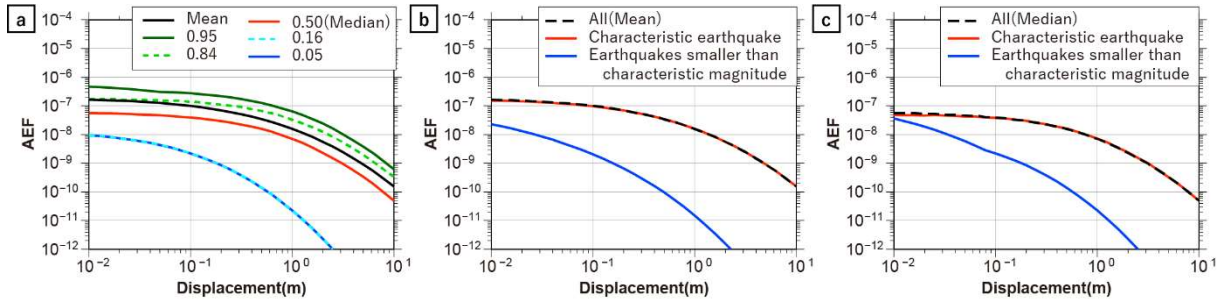
Fig. 9 Fault displacement hazard analysis results. (a) Weighted mean and fractile hazards for all cases. (b), (c) Hazard analysis results for characteristic magnitude earthquakes and earthquakes smaller than characteristic magnitude of active intraplate faults ((b) Mean, (c) Median).
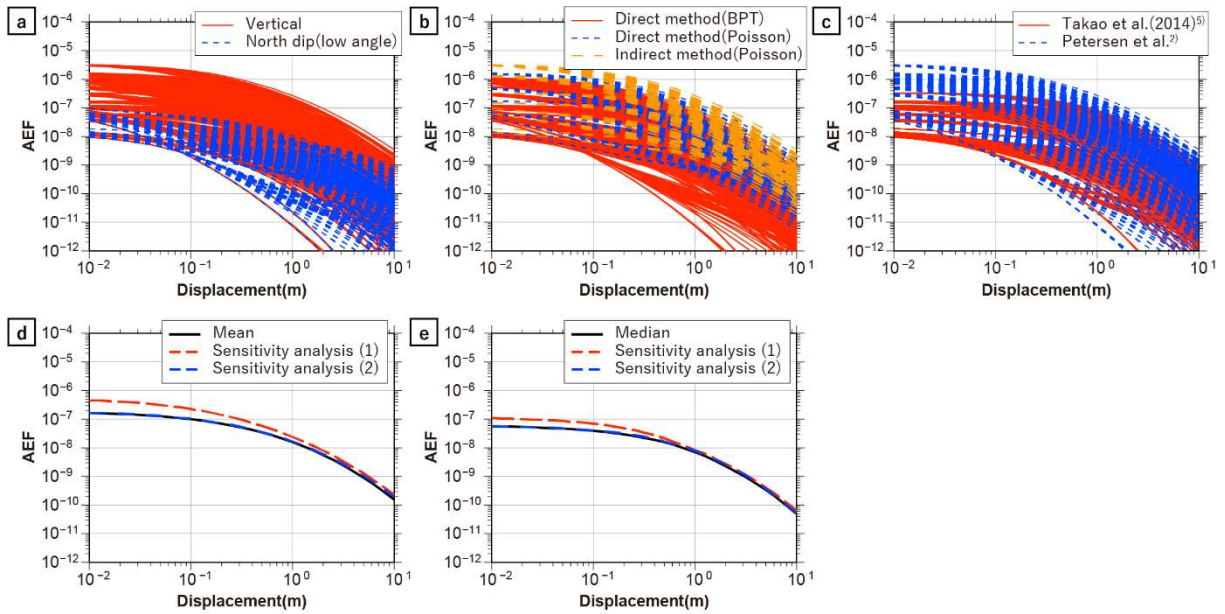

Fig. 10 Sensitivity analysis results. (a) Comparison of hazard curves for branches of fault dip angle at shallow sections. (b) Comparison of hazard curves for branches of time-dependent or time-independent occurrence model. (c) Comparison of hazard curves for branches of the probability of occurrence of the distributed fault (P_{2d}). (d), (e) Comparison of hazard curves when the weights of prediction equations by Takao et al. (2014)[5] and Petersen et al.[2] are changed to 0.5:0.5 (sensitivity analysis case (1)), and when P_{1p} is changed to 0.01 for the case where the shortest distance to the principal fault is approximately 600 m (sensitivity analysis case (2)) ((d) Mean, (e) Median).

4.2 Sensitivity analysis results

Figures 10(a) to 10(c) show comparisons of hazard curves for all branches in the logic tree of the fault dip angle at shallow sections, the time-dependent or time-independent occurrence models, and the probability of occurrence of the distributed fault (P_{2d}), all of which are color-coded according to branch parameter. The branches of the fault dip angle at shallow sections are vertical (90 deg) and north dip (low angle), with the shortest distance from the principal fault at approximately 8 km for the former and approximately 600 m for the latter (Fig. 3). According to Fig. 10(a), the hazard curves for the former, which is farther away from the principal fault, are significantly larger. This is because the probability of occurrence of the principal fault (P_{1p}) is little for the latter, with $P_{1p} = 1$ for the former and $P_{1p} = 0.001$ for the latter. The branches of the time-dependent or time-independent occurrence model includes the

BPT distribution and the Poisson process for the direct method, and the Poisson process for the indirect method, with a mean recurrence interval of 3060 years for the direct method and a shorter interval of 1000 years for the indirect method (Fig. 5). As shown in Fig. 10(b), the hazard curves of the indirect method with a shorter mean recurrence interval are generally larger. This branch parameter significantly affects the probability of earthquake occurrence. The tendency that the parameters involved in calculations of occurrence probability have a significant effect is similar to the PSHA results[15]. For the probability of occurrence of the distributed fault (P_{2d}), the branches are the prediction equations by Takao et al. (2014)[5] and Petersen et al.[2] (Fig. 7). As shown in Fig. 10(c), the former, which was given a larger weight to take their range of applications into account, had significantly smaller hazard curves.

If the weights of the prediction equations by Takao et al. (2014)[5] and Petersen et al.[2] for the probability of occurrence of the distributed fault (P_{2d}) are changed to 0.5:0.5 and the weight of Petersen et al.[2] is increased even though the shortest distance from the principal fault is approximately 8 km, which is essentially outside of its applicable range, both mean and median hazard curves increase significantly (Figs. 10(d) and 10(e)). The results of the sensitivity analysis show that the probability of occurrence of the distributed fault (P_{2d}) has a significant effect on the hazard, and that the adequacy of the prediction equation by Takao et al. (2014)[5], which was given a larger weight, considerably affects the reliability of the PFDHA results. Moreover, when the shortest distance from the principal fault is approximately 600 m, a remarkably small value is set for the probability of occurrence of the principal fault (P_{1p}), with $P_{1p} = 0.001$. However, even if this is increased by an order of magnitude to $P_{1p} = 0.01$, both mean and median hazard curves are almost unchanged (Figs. 10(d) and 10(e)). Based on the interpretation of acoustic exploration records in Fig. 8, we considered it inappropriate to further increase P_{1p} and determined that setting $P_{1p} = 0.001$ poses no problem for evaluating the fault displacement hazard.

5. DISCUSSION OF THE DEVELOPED FAULT DISPLACEMENT CHARACTERIZATION MODEL

5.1 Findings from the 2016 Kumamoto Earthquake observation data

The results of PFDHA and sensitivity analyses show that the choice of fault displacement prediction equation used to set the probability of occurrence of the distributed fault (P_{2d}) has a significant effect on hazard, which is similar to the significant effect on hazard of the choice of ground motion prediction equation in PSHA at the Ikata site[18]. According to Takao et al. (2016)[6], the issue of revising the fault displacement prediction equation to make use of remote sensing techniques that can capture surface crustal deformation remains as a future challenge. For the 2016 Kumamoto Earthquake, interferometric synthetic aperture radar (InSAR) data of crustal deformation on the surface were immediately provided after the earthquake[30]. Moreover, many active fault researchers conducted extensive and detailed ground surveys of surface ruptures (for example, Shirahama et al.[31]). Here, the small displacement lineaments (DL) detected by InSAR include displacements caused by faults that do not reach the surface (Fujiwara et al.[32]). In this paper, following the approach by Takao et al. (2014)[5], we consider surface ruptures identified onsite as hazards. Using the final compilation of surface rupture distributions by university research groups in Kumahara et al.[33], and referring to the 1:25000-scale Active Fault Map in Urban Areas by the Geospatial Information Authority of Japan (GSI)[34, 35] and the survey results by the National Institute of Advanced Industrial Science and Technology[31], we compiled observation data on surface rupture distribution of the 2016 Kumamoto Earthquake and studied the validity of the probability of occurrence of the distributed fault (P_{2d}) proposed by Takao et al, (2014)[5] to which we had given a large weight and used in this paper.

Figure 11(a) shows the active fault distribution and Fig. 11(b) shows the surface rupture distribution at the 2016 Kumamoto Earthquake focal region. The 2016 Kumamoto Earthquake was a Mw 7.0 earthquake that occurred at the Futagawa fault and the northernmost part of the Hinagu fault with predominantly right-lateral strike-slip[33]. The surface rupture distribution of the 2016 Kumamoto Earthquake was remarkably complex, making it difficult to clearly distinguish the principal fault, which

was defined as the fault closely related to the earthquake source fault in Takao et al. (2014)[5], from other distributed faults. Asano and Iwata[36] had shown that the shallower portion of the earthquake source fault contributed to the velocity and displacement waveforms near the fault. In this paper, focusing on the fact that the fault displacement sense is that of a right-lateral strike-slip, we identified the fault near the upper end of the earthquake source fault by Asano and Iwata[36] as the principal fault (Fig. 11(b)). Here, the Idenokuchi fault, which runs parallel to the Futagawa fault on its southeast side for about 2 km, has a predominant normal fault component. However, its maximum displacement is nearly the same as that of the Futagawa fault, and a proposed model shows that normal fault displacement is taken up by the surface on the extension line from the earthquake source fault (Toda et al.[37]). Hence, there are suggestions that the Idenokuchi fault is the principal fault. But since there is a separation from the upper end of the earthquake source fault according to Asano and Iwata[36], it is treated as a distributed fault in this paper. The epistemic uncertainty of classifying surface ruptures into the principal fault and distributed faults is a major challenge in the current PFDHA. Additionally, the Suizenji fault (Goto et al.[38]), the Kuradake fault group (Sato et al.[39]), and the Miyaji fault (Ishimura et al.[40]) are thought to have triggered displacements far away from the principal fault during the 2016 Kumamoto Earthquake (Fig. 11). For the most part, the fault displacements are thought to have occurred in fault planes that have been repeatedly ruptured in the past. With the exception of the Miyaji fault located in an alluvial fan, these are active faults that have been recognized in tectonic geomorphology studies.
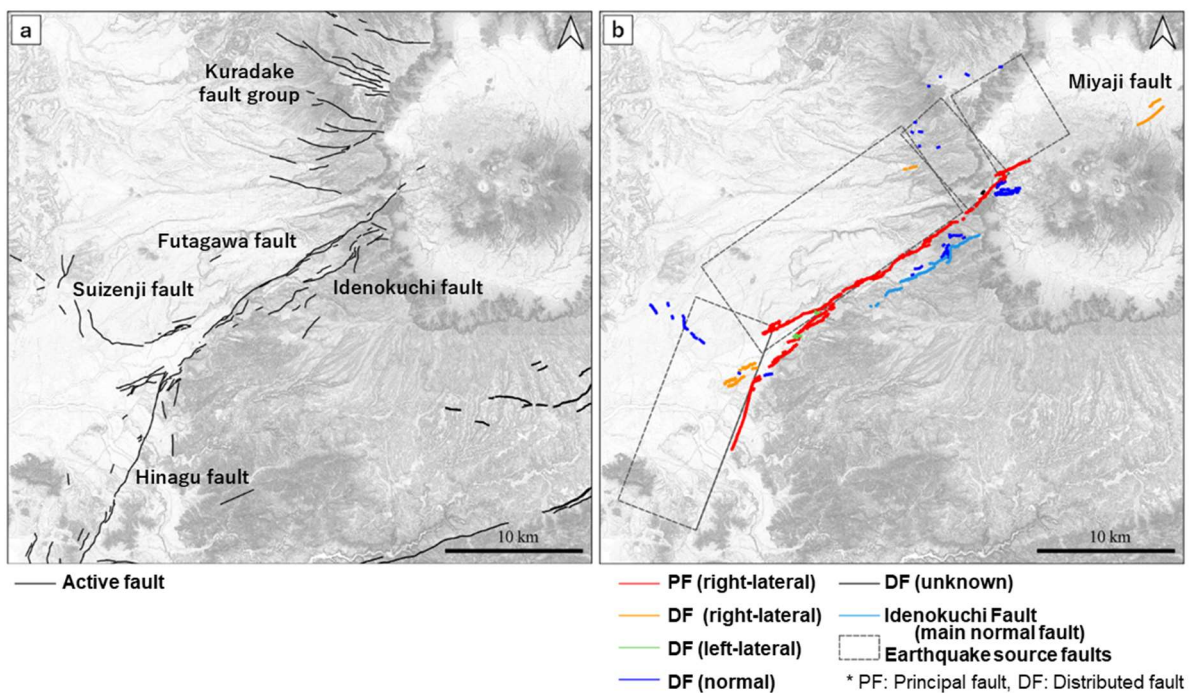

Fig. 11 Fault distribution at the 2016 Kumamoto Earthquake focal region. (a) Active fault distribution. Created based on the 1:25000-scale Active Fault Map in Arban Areas by GSI[34, 35] and referencing the Digital Active Fault Map of Japan[41]. (b) Surface rupture distribution. Created based on Kumahara et al.[33] and referencing the 1:25000-scale Active Fault Map in Arban Areas by GSI[34, 35] and Shirahama et al.[31]. Earthquake source faults is referred from Asano and Iwata[36].

To analyze the surface ruptures that occurred far from the principal fault, we plotted the probability of occurrence of the distributed fault according to the distance from the principal fault with a grid size of 250 m x 250 m based on the 2016 Kumamoto Earthquake observation data (Fig. 11(b)) and performed a logistic regression to compare it with the prediction equation by Takao et al. (2014)[5] (Fig. 12). Here, we used data from up to 25 km away from the principal fault, following the example by Takao et al. (2014)[5]. The regression equation for distributed faults based on the 2016 Kumamoto Earthquake

observation data gave generally higher values than the prediction equation by Takao et al. (2014)[5] and the divergence between the two is particularly noticeable at a distance of more than 3 km from the principal fault. If the main normal fault in the Idenokuchi fault distribution region according to Kumahara et al.[33] is treated as the principal fault, the probability of occurrence of the distributed fault is significantly reduced, but the deviation from the prediction equation by Takao et al. (2014)[5] remains in distant regions. In a preliminary report, Takao et al.[42] showed that the inclusion of observation data from the 2016 Kumamoto Earthquake did not have a significant effect on the prediction equation, and that a reevaluation will be needed to include survey developments made far from the principal fault. Since then, it is thought that the impact of data reported for the Kuradake fault group and the Miyaji fault may have caused the divergence.
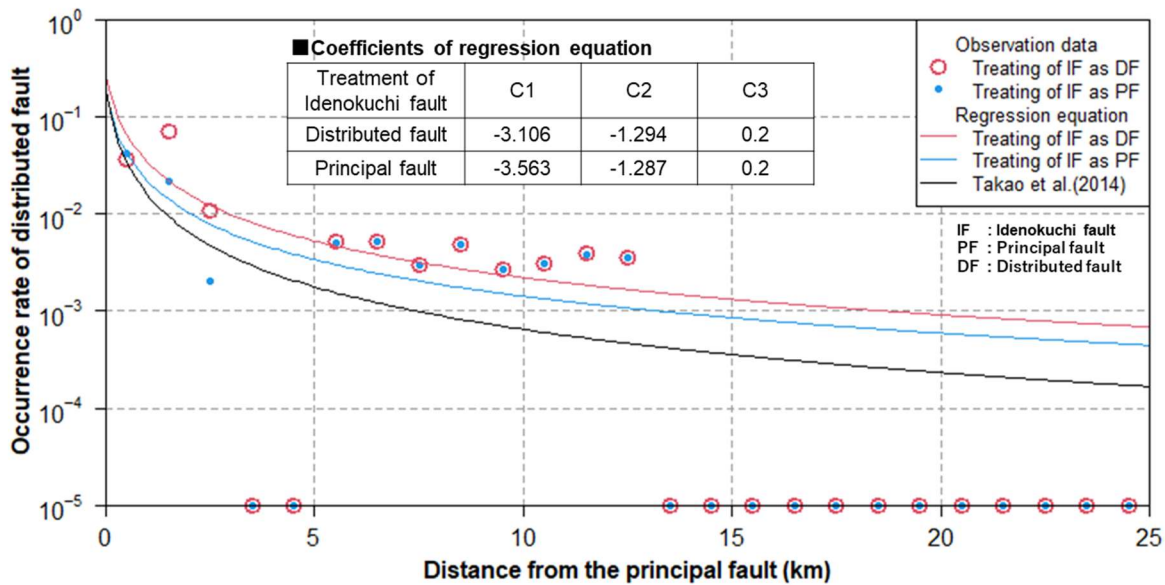

Fig. 12 Comparison of the probability of occurrence of the distributed fault caused by the 2016 Kumamoto Earthquake with distance from the principal fault and the probability of occurrence of the distributed fault based on the prediction equation by Takao et al.(2014)[5] (P_{2d}). Plotted using a grid size of 250 m x 250 m.

The prediction equation by Takao et al. (2014)[5] was formulated based on the assumption that the probability of occurrence of the distributed fault is uniform in all directions. However, based on the 2016 Kumamoto Earthquake observation data (Fig. 11(b)), the distribution of remote distributed faults appears to be skewed toward the northwestern side of the principal fault. To verify the uneven distribution of distributed faults quantitatively, the percentages of the direction of appearance (divided into northwestern side, southeastern side, and eastward extended region from the principal fault) and the displacement sense of distributed faults with distance from the principal fault were graphically illustrated (Fig. 13). A large percentage of distributed faults with a normal fault sense originated in the southeastern side of up to a distance of 3 km from the principal fault, whereas distributed fault with a left-lateral sense was observed only within a distance of 1 km from the principal fault. At a distance of 1 to 3 km, about 80 % are normal faults on the southeastern side, which correspond to the Idenokuchi fault running parallel to the Futagawa fault on its southeastern side for approximately 2 km. There is no distributed fault at a distance of 3 to 5 km from the principal fault. Moreover, there is no distributed fault beyond 5 km on the southeastern side. Distributed faults with a right-lateral sense at 5 to 7 km from the principal fault on the northwestern side are shown as presumed active faults on the Active Fault Map in Urban Areas[35]. Distributed faults with a normal fault sense at 5 to 11 km from the principal fault on the northwestern side correspond to the Suizenji fault and the Kuradake fault group. In addition, distributed faults with a right-lateral sense at 10 to 13 km from the principal fault on the eastward extended region

correspond to the Miyaji fault. Therefore, all the distributed ruptures that occurred at distances over 3 km from the principal fault in the 2016 Kumamoto Earthquake are believed to be related to existing active faults. Based on the above, the uneven distribution of distributed faults on the northwestern side or the eastward extended region further away from the principal fault may mainly be attributed to the following factors: existing active faults that triggered fault displacements can be occurred during earthquakes, static stress changes due to being located on a hanging wall or on the extended region of the northwest-dipping earthquake source fault at 60 to 90 deg[36)], or dynamic stress changes due to seismic motions on the northwestern side where there is a wide region of soft soil layer or within the Aso caldera, rather than on the southeastern side with hard bedrock on a mountainous region (Fig. 11). The events that can serve as a cause or trigger likely affect each other in a complex manner and studying how they do so is a topic for further studies.
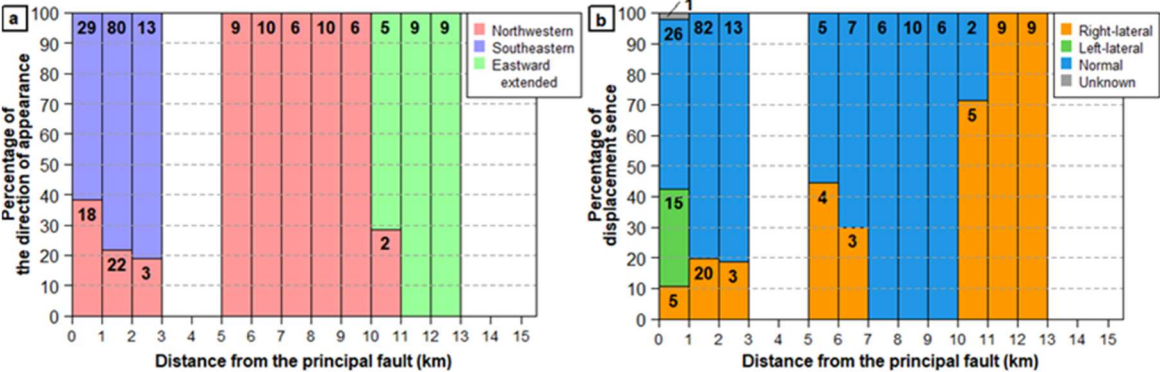

Fig. 13 Percentage of distributed faults caused by the 2016 Kumamoto Earthquake with distance from the principal fault. Numbers in the bar graph indicate frequency (number of grids). (a) Percentage of direction of appearance of distributed faults. Divided into three sections from the principal fault: northwestern side, southeastern side, and eastward extended. (b) Percentage of displacement sense of distributed faults.

5.2   Issues with the fault displacement characterization model at the Ikata site

Since the Ikata site is located approximately 8 km from the closest point of the principal fault on the long and highly active MTLAFZ, a fault displacement prediction equation that can accurately calculate the probability of occurrence of the distributed fault (P_{2d}) at relevant distances is essential for ensuring the reliability of the fault displacement hazard analysis. However, there are only two widely used prediction equations for distributed faults caused by strike-slip faults—the equations by Takao et al. (2014)[5)] and by Petersen et al.[2)]. Furthermore, the latter is recommended for application in cases only up to 2 km away from the principal fault, so only the former prediction equation is applicable to distances farther away from the principal fault. Takao et al. (2014)[5)] used 19 earthquakes—from the 1891 Nobi earthquake to the 2008 Iwate–Miyagi earthquake—to formulate a prediction equation for the probability of occurrence of the distributed fault (P_{2d}). As pointed out in Takao et al. (2016)[6)], there is a lack of data on distant fault displacements because surveys have mainly been carried out over areas relatively close to the principal fault. The observation data on the 2016 Kumamoto Earthquake, for which detailed surveys were conducted over a wide area has an obvious divergence as mentioned in the previous section. The 2016 Kumamoto Earthquake contains large amounts of normal fault components at the southern edge of the Beppu–Shimabara rift zone, and may potentially have different characteristics from the 19 earthquakes used in formulating the prediction equation by Takao et al. (2014)[5)]. Going forward, there is a need to expand fault displacement data to include data at greater distances away from the principal fault by not only using observation data of actual earthquakes but also by using numerical analysis and other methods.

In the prediction equation by Takao et al. (2014)[5)], the only explanatory variable for calculating the probability of occurrence of the distributed fault (P_{2d}) is the distance from the principal fault. In the

process of formulating the prediction equation, the presence of existing active faults at rupture sites was not taken into account. Moreover, the presence of active faults at the assessed site was not taken into account during the evaluation as well. Takao et al. (2014)[5] reasoned that they did not consider the presence of existing active faults at locations where distributed fault appeared because their aim was to study and arrive at a general application of PFDHA and not for specific structures. However, locations for nuclear power plants undergo exhaustive investigations to make sure they avoid sites with a risk of fault displacements. Meanwhile, surface ruptures that occurred far from the principal fault during the 2016 Kumamoto Earthquake are all believed to be related to existing active faults. Aside from the 2016 Kumamoto Earthquake, many other cases of triggered surface ruptures along existing active faults have been found in and out of Japan[43), 44]. The rise in fault displacement hazard due to small but frequent surface ruptures in short active faults has been discussed[43), 45]. The series of studies by Takao et al.[4)–6] had led to the publication of the AESJ Standards[7]; in light of the growing demand for studies targeting specific structures far from the principal fault, as in this paper, we may now have entered the stage where a fault displacement prediction equation that can take into account the presence of existing active faults at sites where fault displacements occurred and at the site under study must be established.

Focusing on the active fault distribution around the Ikata site, the active fault density is higher on the northwestern side (inner zone) than on the southeastern side (outer zone) of the MTLAFZ (Fig. 1), similar to the source region of the 2016 Kumamoto Earthquake (Fig. 11). These regional characteristics of active fault distribution are compiled in seismotectonic province maps typified by the work of Kakimi et al.[46]. Toda[47] explains that the reason why there are few active faults at the outer zone of southwestern Japan is because local strain release is efficiently taken up mainly by the plate boundaries, whereas the inner zone has a system in which multiple active faults accumulate long-term strain inefficiently. Furthermore, in the model of seismic source characteristics in this paper, the dip angles of the earthquake source fault at the MTLAFZ were set with weights of 0.5:0.5 for vertical (90 deg) and north-dipping (40 deg) faults (Fig. 3). The latter is based on the assumption that the active fault with high-angle at the shallow section does not cut the mid-angled MTL geological boundary at the deep section into the Sambagawa metamorphic rocks. Since the assumption means that the strength and friction coefficient of the MTL as a geological boundary are smaller than those of other faults, the earthquake source fault would coincide with the geological boundary[14], and if this is the case, distributed ruptures would be unlikely to occur in the solid Sambagawa metamorphic rocks composing the footwall. In the future, we hope to see the development of a method that can take into account such site-specific seismotectonics.

6. CONCLUSIONS

Passing through approximately 8 km north of the Ikata site located in northwestern Shikoku, the MTLAFZ is a long active fault zone mainly composed of right-lateral strike-slip faults. As the first application of the guidelines for SSHAC Level 3 in Japan, the Ikata SSHAC Project created a highly reliable model of seismic source characteristics at the Ikata site. In this paper, we utilized this model as well as constructed a fault displacement characterization model considering the opinions of experts in relevant fields and implemented PFDHA. The results of the PFDHA showed that when activity of the MTLAFZ (Iyo-nada Segment) is considered, the annual frequency of fault displacements occurring directly below critical seismic-resistant facilities at the Ikata site is about 1×10^{-7}. Moreover, for displacements over 0.1 m, the AEF progressively declines with increase in displacement. Furthermore, for fault displacement hazard, the effect of characteristic earthquakes dominates, and as the displacement increases, the hazard curve diverges greatly from the hazard curve of earthquakes smaller than characteristic magnitude of active intraplate faults. Results of sensitivity analyses show that, similar to the PSHA results, parameters involved in calculating the probability of earthquake occurrence have a significant effect, and that the choice of fault displacement prediction equation used to set the probability of occurrence of the distributed fault has a significant effect on hazard, which is also similar to the choice of ground motion prediction equation in the PSHA. All of the distributed ruptures that occurred at distances over 3 km from the principal fault in the 2016 Kumamoto Earthquake are believed to be related to existing active faults. Hence, the issues that need to be resolved to practically use PFDHA include

expanding fault displacement data to include data at greater distances away from the principal fault, establishing a fault displacement prediction equation that can take into account the presence of existing active faults, and developing a method that can take into account site-specific seismotectonics. We believe that the knowledge gained by fully implementing PFDHA at the Ikata site, the first study of its kind on a specific structure in Japan, will greatly contribute to the future development of PFDHA.

ACKNOWLEDGMENT

APPENDIX 1: FAULT DISPLACEMENT PREDICTION EQUATION FOR DISTRIBUTED FAULT

The earthquake approach procedure for PFDHA is described in detail by Youngs et al.[1] and is summarized by Takao et al. (2013)[4]. According to Takao et al. (2013)[4], the probability that the distributed fault displacement D will exceed d at the shortest distance r from the principal fault of length L is expressed by Eq. (A-1) below, and the AEF of distributed fault displacements is evaluated as the product of Eq. (A-1) and the annual frequency of the active fault.

$$P_d (D > d \mid m, r, L) = P_{lp} (PF \mid m) \times P_{2d} (Slip \mid m, r, PF) \times P_{3d} (D > d \mid m, r, Slip) \qquad \text{(A-1)}$$

$P_{lp} (PF \mid m)$: Probability that the principal fault rupture will reach the surface for an earthquake of magnitude m. PF refers to the principal fault.

$P_{2d} (Slip \mid m, r, PF)$: Probability that the distributed fault displacement will appear at distance r from the principal fault. $Slip$ refers to the fault displacement.

$P_{3d} (D > d \mid m, r, Slip)$: Probability that the fault displacement D will exceed d when the distributed fault displacement appears at distance r.

APPENDIX 2: COMPARISON OF FAULT DISPLACEMENT PREDICTION EQUATIONS FOR DISTRIBUTED FAULT CAUSED BY STRIKE-SLIP FAULTS

In this paper, we used the prediction equations by Petersen et al.[2] and Takao et al. (2014)[5] for the probability of occurrence of the distributed fault (P_{2d}) to account for distributed faults caused by strike-slip faults. In both equations, the farther away from the principal fault, the lower the probability of occurrence of the distributed fault, and the former equation yields higher rates than the latter (Fig. A-1(a)). On the other hand, the amount of displacement of distributed faults is given by a normalized prediction equation with respect to the principal fault displacement. In this paper, we used the prediction equations by Petersen et al.[2] and Takao et al. (2016)[6]. In both equations, the farther away from the principal fault, the lower the displacement of distributed faults, although the latter equation yields higher displacements (Fig. A-1(b)).
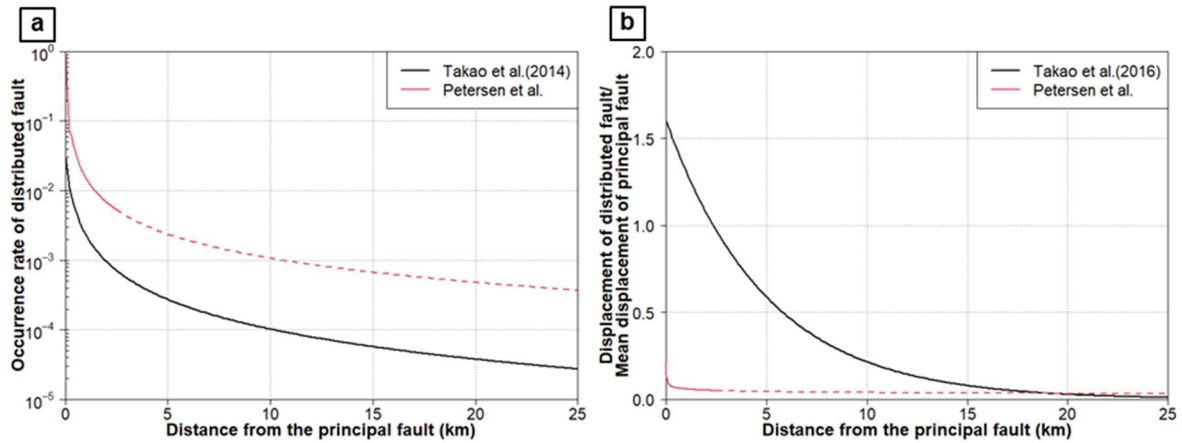
Fig. A-1 Comparison of fault displacement prediction equations for distributed faults caused by strike-slip faults. (a) Comparison of occurrence rate of distributed fault between the prediction equations by Petersen et al.[2] and Takao et al. (2014)[5]. After calculating with the prediction equation by Petersen et al.[2] using a grid size of 200 m x 200 m and with the prediction equation by Takao et al. (2014)[5] using 250 m x 250 m, the results were calibrated with an area ratio for 160 m x 160 m. (b) Comparison of distributed fault displacements between the prediction equations by Petersen et al.[2] and Takao et al. (2016)[6].

REFERENCES

1) Youngs, R. R., Arabasz, W. J., Anderson, R. E., Ramelli, A. R., Ake, J. P., Slemmons, D. B., McCalpin, J. P., Doser, D. I., Fridrich, C. J., Swan III, F. H., Rogers, A. M., Yount, J. C., Anderson, L. W., Smith, K. D., Bruhn, R. L., Knuepfer, P. L. K., Smith, R. B., dePolo, C. M., O'Leary, D. W., Coppersmith, K. J., Pezzopane, S. K., Schwartz, D. P., Whitney, J. W., Olig, S. S. and Toro, G. R.: A Methodology for Probabilistic Fault Displacement Hazard Analysis (PFDHA), *Earthquake Spectra*, Vol. 19, No. 1, pp. 191–219, 2003.

2) Petersen, M. D., Dawson, T. E., Chen, R., Cao, T., Wills, C. J., Schwartz, D. P. and Frankel, A. D.: Fault Displacement Hazard for Strike-Slip Faults, *Bulletin of the Seismological Society of America*, Vol. 101, No. 2, pp. 805–825, 2011.

3) Moss, R. E. S. and Ross, Z. E.: Probabilistic Fault Displacement Hazard Analysis for Reverse Faults, *Bulletin of the Seismological Society of America*, Vol. 101, No. 4, pp. 1542–1553, 2011.

4) Takao, M., Tsuchiyama, J., Annaka, T. and Kurita, T.: Application of Probabilistic Fault Displacement Hazard Analysis in Japan, *Journal of Japan Association for Earthquake Engineering*, Vol. 13, No. 1, pp. 17–36, 2013 (in Japanese).

5) Takao, M., Ueta, K., Annaka, T., Kurita, T., Nakase, H., Kyoya, T. and Kato, J.: Reliability Improvement of Probabilistic Fault Displacement Hazard Analysis, *Journal of Japan Association for Earthquake Engineering*, Vol. 14, No. 2, pp. 16–36, 2014 (in Japanese).

6) Takao, M., Tani, T., Oshima, T., Annaka, T. and Kurita, T.: Maximum Likelihood Estimation of the Parameters Regarding Displacement Evaluation of Distributed Fault in PFDHA, *Journal of Japan Association for Earthquake Engineering*, Vol. 16, No. 2, pp. 96–101, 2016 (in Japanese).

7) Atomic Energy Society of Japan: A Standard for Procedure of Fault Displacement Probabilistic Risk Assessment for Nuclear Power Plants: 2021 (AESJ-SC-RK009:2021), 306 pp., 2021 (in Japanese).

8) International Atomic Energy Agency: Seismic Hazards in Site Evaluation for Nuclear Installations, No. DS507, Revision of Safety Guide SSG-9, 78 pp., 2022.

9) International Atomic Energy Agency: An Introduction to Probabilistic Fault Displacement Hazard Analysis in Site Evaluation for Existing Nuclear Installations, IAEA-TECDOC-1987, 134 pp.,

2021.

10) Valentini, A., Fukushima, Y., Contri, P., Ono, M., Sakai, T., Thompson, S.C., Viallet, E., Annaka, T., Chen, R., Moss, R. E. S., Petersen, M. D., Visini, F. and Youngs, R. R.: Probabilistic Fault Displacement Hazard Assessment (PFDHA) for Nuclear Installations According to IAEA Safety Standards, *Bulletin of the Seismological Society of America*, Vol. 111, No. 5, pp. 2661–2672, 2021.

11) Inoue, N., Kitada, N., Shibuya, N., Omata, M., Takahama, T., Tonagi, M. and Irikura, K.: Probabilistic Evaluation of Off-Fault Displacements of the 2016 Kumamoto Earthquake, *Pure and Applied Geophysics*, Vol. 177, pp. 2007–2019, 2020.

12) The United States Nuclear Regulatory Commission: Practical Implementation Guidelines for SSHAC Level 3 and 4 Hazard Studies, The United States Nuclear Regulatory Commission NUREG-2117, Rev. 1, 141 pp., 2012.

13) The United States Nuclear Regulatory Commission: Updated Implementation Guidelines for SSHAC Hazard Studies, The United States Nuclear Regulatory Commission NUREG-2213, 145 pp., 2018.

14) Kameda, H., Kumamoto, T., Fujiwara, H., Okumura, K., Tsukuda, E., Tsutsumi, H., Tsutsumi, H., Toda, S., Tokuyama, H., Ebisawa, K., Kagawa, T., Si, H., Furumura, T., Miyake, H., Morikawa, N., Okumura, T. and Miyakoshi, J.: Ikata SSHAC Project Final Report, 2020 (in Japanese). https://www.yonden.co.jp/energy/atom/safety/sshac_project/index.html (last accessed on February 1, 2023)

15) Kumamoto, T., Okumura, K., Tsukuda, E., Tsusumi, H., Tsutsumi, H., Toda, S., Tokuyama, H., Onishi, K., Nishizaka, N., Ohno, Y., Sakai, T. and Kameda, H.: Development of Model of Seismic Source Characteristics at the Ikata Site Based on Guidelines for SSHAC Level 3, *Journal of Japan Association for Earthquake Engineering*, Vol. 22, No. 2, pp. 37–60, 2020 (in Japanese).

16) Earthquake Research Committee, Headquarters for Earthquake Research Promotion: Long-Term Evaluation Methodology for Active Faults (Tentative Version), 2010 (in Japanese, title translated by the authors). https://www.jishin.go.jp/main/choukihyoka/katsu_hyokashuho/index.htm (last accessed on February 1, 2023)

17) Toda, S.: *To What Extent Can Active Fault Earthquakes Be Predicted?*, Blue Backs, 287 pp., 2016 (in Japanese, title translated by the authors).

18) Fujiwara, H., Ebisawa, K., Kagawa, T., Si, H., Furumura, T., Miyake, H., Morikawa, N., Shiota, T., Ogawa, H., Matsusaki, S., Miyakoshi, J., Sakai, T. and Kameda, H.: Development of Ground Motion Characterization Model at the Ikata Site Based on Guidelines for SSHAC Level 3, *Journal of Japan Association for Earthquake Engineering*, Vol. 22, No. 2, pp. 61–87, 2022 (in Japanese).

19) Japan Society of Civil Engineers: *Evaluation Techniques for Active Fault Systems in Nuclear Power Plants—Segmentation of Long Active Fault Systems—*, 175 pp., 2004 (in Japanese, title translated by the authors).

20) Wells, D. L. and Coppersmith, K. J.: New Empirical Relationships among Magnitude, Rupture Length, Rupture Width, Rupture Area, and Surface Displacement, *Bulletin of the Seismological Society of America*, Vol. 84, No. 4, pp. 974–1002, 1994.

21) Somerville, P., Irikura, K., Graves, R., Sawada, S., Wald, D., Abrahamson, N., Iwasaki, Y., Kagawa, T., Smith, N. and Kowada, A.: Characterizing Crustal Earthquake Slip Models for the Prediction of Strong Ground Motion, *Seismological Research Letters*, Vol. 70, No. 1, pp. 59–80, 1999.

22) Irikura, K. and Miyake, H.: Prediction of Strong Ground Motions for Scenario Earthquakes, *Journal of Geography*, Vol. 110, No. 6, pp. 849–875, 2001 (in Japanese).

23) Murotani, S., Matsushima, S., Azuma, T., Irikura, K. and Kitagawa S.: Scaling Relations of Source Parameters of Earthquakes Occurring on Inland Crustal Mega-fault Systems, *Pure and Applied Geophysics*, Vol. 172, pp. 1371–1381, 2015.

24) Leonard, M.: Self-Consistent Earthquake Fault-Scaling Relations: Update and Extension to Stable Continental Strike-Slip Faults, *Bulletin of the Seismological Society of America*, Vol. 104, No. 6, pp. 2953–2965, 2014.

25) Earthquake Research Committee, Headquarters for Earthquake Research Promotion: National Seismic Hazard Maps for Japan (2016), 2016 (in Japanese). https://www.jishin.go.jp/evaluation/seismic_hazard_map/shm_report/ (last accessed on February 1,

2023)

26) Working Group on California Earthquake Probabilities: Earthquake Probabilities in the San Francisco Bay Region: 2002–2031, *U.S. Geological Survey*, Open-File Report 03-214, 235 pp., 2003. https://pubs.er.usgs.gov/publication/ofr03214 (last accessed on February 1, 2023)

27) Takahashi, K., Ikeda, M., Sato, T., Adachi, K., Nishizaka, N., Onishi, K., Ohno, Y., Tsuyuguchi, K. and Tsuji, T.: Distribution and Activity of Median Tectonic Line in the Iyo-Nada Sea off Northwestern Shikoku Based on Seismic Survey, *Active Fault Research*, Vol. 53, pp. 13–32, 2020 (in Japanese).

28) Research Group for Active Faults of Japan (Eds.): *Active Fault in Japan (Revised Edition)*, University of Tokyo Press, 437 pp., 1991 (in Japanese).

29) U.S. Nuclear Regulatory Commission: Confirmatory Analysis of Seismic Hazard at the Diablo Canyon Power Plant from the Shoreline Fault Zone, Research Information Letter 12-01, pp. C1–C23, 2012. https://www.nrc.gov/docs/ML1212/ML121230035.pdf (last accessed on May 1, 2023)

30) Fujiwara, S., Yarai, H., Kobayashi, T., Morishita, Y., Nakano, T., Miyahara, B., Nakai, H., Miura, Y., Ueshiba, H., Kakiage, Y. and Une, H.: Small-Displacement Linear Surface Ruptures of the 2016 Kumamoto Earthquake Sequence Detected by ALOS-2 SAR, *Earth, Planets and Space*, Vol. 68, 160, pp. 1–17, 2016.

31) Shirahama, Y., Yoshimi. M., Awata, Y., Maruyama, T., Azuma, T., Miyashita, Y., Mori, H., Imanishi, K., Takeda, N., Ochi, T., Otsubo, M., Asahina, D. and Miyakawa, A.: Characteristics of the Surface Ruptures Associated with the 2016 Kumamoto Earthquake Sequence, Central Kyushu, Japan, *Earth, Planets and Space*, Vol. 68, 191, pp. 1–12, 2016.

32) Fujiwara, S., Nakano, T. and Morishita, Y.: Detection of Triggered Shallow Slips Caused by Large Earthquakes Using L-Band SAR Interferometry, *Earth, Planets and Space*, Vol. 72, 119, pp. 1–23, 2020.

33) Kumahara, Y., Kaneda, H., Tsutsumi, H. (eds.): *Surface Ruptures Associated with the 2016 Kumamoto Earthquake Sequence in Southwest Japan*, Springer Singapore, 241 pp., 2022.

34) Kumahara, Y., Okada, S., Kagohara, K., Kaneda, H., Goto, H. and Tsutsumi, H.: 1:25,000-Scale Active Fault Map in Urban Areas "Kumamoto Revised Version", *Geospatial Information Authority of Japan*, D1-No. 868, No. 182, 2017 (in Japanese).

35) Suzuki, Y., Ishimura, D., Kumaki, Y., Kumahara, Y., Chida, N., Nakata, T. and Nakano, T.: 1:25,000-Scale Active Fault Map in Urban Areas "Aso", *Geospatial Information Authority of Japan*, D1-No. 868, No. 181, 2017 (in Japanese).

36) Asano, K. and Iwata, T.: Revisiting the Source Rupture Process of the Mainshock of the 2016 Kumamoto Earthquake and Implications for the Generation of Near-Fault Ground Motions and Forward-Directivity Pulse, *Bulletin of the Seismological Society of America*, Vol. 111, No. 5, pp. 2426–2440, 2021.

37) Toda, S., Kaneda, H., Okada, S., Ishimura, D. and Mildon, Z.K.: Slip-Partitioned Surface Ruptures for the Mw 7.0 16 April 2016 Kumamoto, Japan, Earthquake, *Earth, Planets and Space,* Vol. 68, 188, pp. 1–11, 2016.

38) Goto, H., Tsutsumi, H., Toda, S. and Kumahara, Y.: Geomorphic Features of Surface Ruptures Associated with the 2016 Kumamoto Earthquake in and around the Downtown of Kumamoto City, and Implications on Triggered Slip along Active Faults, *Earth, Planets and Space*, Vol. 69, 26, pp. 1–12, 2017.

39) Sato, H. P., Komura, K., Une, H., Nakano, T. and Yagi, H.: Study on Cumulative Activities of Passively Ruptured Faults through a Trenching Survey at the Matoishi Bokujo I Fault, Northwest Side of the Aso Caldera, Southwestern Japan, *Geographical Review of Japan Series A*, Vol. 94, No. 4, pp. 250–264, 2021 (in Japanese).

40) Ishimura, D., Tsutsumi, H., Toda, S., Fukushima, Y., Kumahara, Y., Takahashi, N., Ichihara, T. and Takada, K.: Repeated Triggered Ruptures on a Distributed Secondary Fault System: an Example from the 2016 Kumamoto Earthquake, Southwest Japan, *Earth, Planets and Space*, Vol. 73, 39, pp. 1–17, 2021.

41) Nakata, T. and Imaizumi, T. (Eds.): *Digital Active Fault Map in Japan*, University of Tokyo Press, 2002 (in Japanese).

42) Takao, M., Kaneto, T. and Kurita, T.: Outline of the PFDHA Method and Recent Studies on PFDHA in Japan, *Second Workshop on Best Practices in Physics-Based Fault Rupture Models for Seismic Hazard Assessment of Nuclear Installations: Issues and Challenges Towards Full Seismic Risk Analysis*, International Atomic Energy Agency, Cadarache-Château, France, pp. 1–14, 2018.

43) Toda, S. and Ishimura, D.: Evaluation of Short Active Faults Reflected from Distributed Minor Surface Breaks Found at Recent Inland Large Earthquakes Including the 2016 Kumamoto Earthquake, *The Quaternary Research*, Vol. 58, pp. 121–136, 2019 (in Japanese).

44) Parsons, T., Geist, E. L. and Parsons, S. E.: "Aftershock Faults" and What They Could Mean for Seismic Hazard Assessment, *The Seismic Record*, Vol. 3, No. 1, pp. 1–11, 2023.

45) Takada, T. and Itoi, T.: Approaches to Ensure Nuclear Safety to Face Risks of Seismic Faults: Reports on the AESJ 2018 Special International Symposium, *Journal of the Atomic Energy Society of Japan*, Vol. 60, No. 12, pp. 770–775, 2018 (in Japanese).

46) Kakimi, T., Matsuda, T., Aida, I. and Kinugasa, Y.: A Seismotectonic Province Map in and around the Japanese Islands, *Zisin 2nd ser.*, Vol. 55, pp. 389–406, 2003 (in Japanese).

47) Toda, S.: Current Issues and a Prospective View to the Next Step for Long-Term Crustal Earthquake Forecast in Japan, *The Journal of the Geological Society of Japan*, Vol. 119, pp. 105–123, 2013 (in Japanese).